



U.S. Department  
of Transportation

**National Highway  
Traffic Safety  
Administration**



---

DOT HS 812 786

February 2020

# **Li-Ion Battery Propagation Trigger Technique Development/ Igniter Development**

## DISCLAIMER

This publication is distributed by the U.S. Department of Transportation, National Highway Traffic Safety Administration, in the interest of information exchange. The opinions, findings and conclusions expressed in this publication are those of the authors and not necessarily those of the Department of Transportation or the National Highway Traffic Safety Administration. The United States Government assumes no liability for its contents or use thereof. If trade or manufacturers' names are mentioned, it is only because they are considered essential to the object of the publication and should not be construed as an endorsement. The United States Government does not endorse products or manufacturers.

Suggested APA Format Citation:

Lamb, J., Ko, J., Torres-Castro, L., Stanley, J., Christopher Grosso, C., & Gray, L. (2020, February). *Li-ion battery propagation trigger technique development/igniter development* (Report No. DOT HS 812 786). Washington, DC: National Highway Traffic Safety Administration.

<b>1. Report No.</b> DOT HS 812 786		<b>2. Government Accession No.</b>		<b>3. Recipient's Catalog No.</b>	
<b>4. Title and Subtitle</b> Li-Ion Battery Propagation Trigger Technique Development/Igniter Development				<b>5. Report Date</b> February 2020	
				<b>6. Performing Organization Code</b>	
<b>7. Authors</b> Joshua Lamb, Jonathan Ko, Loraine Torres-Castro, June Stanley, Christopher Grosso and Lucas Gray				<b>8. Performing Organization Report No.</b>	
<b>9. Performing Organization Name and Address</b> Sandia National Laboratories 1515 Eubank SE. Albuquerque, New Mexico 87123				<b>10. Work Unit No. (TRAIS)</b>	
				<b>11. Contract or Grant No.</b>	
<b>12. Sponsoring Agency Name and Address</b> National Highway Traffic Safety Administration 1200 New Jersey Avenue SE Washington, DC 20590				<b>13. Type of Report and Period Covered</b> Interim Report	
				<b>14. Sponsoring Agency Code</b>	
<b>15. Supplementary Notes</b>					
<b>16. Abstract</b> This interim report for single-cell thermal runaway initiator activities performed at Sandia National Laboratories looks at novel initiation methods applied to initiate or simulate failure of a single-cell test. Specifically, it explores first initiation with a high-intensity, undirected quartz lamp. This successfully initiated thermal runaway in pouch cells. However, energy input to the cell was needed and this method was found to only be applicable with the large face of prismatic and pouch cells, limiting the convenience of the technique. As increasingly complex lithium-ion systems are used, concern has arisen surrounding thermal runaway propagation, specifically that a random field failure of a single cell could cause cascading failure of other nearby, otherwise healthy, batteries that ultimately consumes a significant portion of the system. Testing to date has largely focused on single-cell initiation using traditional abuse test methods. However, these methods raise concerns either with the amount of impact to the overall system, or the difficulty in performing the test in a pack outside of a research and development setting. Testing was also performed to develop a contained thermite test device. Commercial thermite materials tested at NSWC Carderock successfully initiated thermal runaway within a single cell. However, to limit impact to the surrounding system, a contained testing device is desired. For this reason, pellets were compacted inside tungsten crucibles and tested to obtain the desired containment and thermite reaction. However, to date no crucibles tested have could fully contain the thermite reaction, making this technique difficult outside of specialized testing laboratories. Ongoing work will make a final determination of the feasibility of a sealed thermite test device. Proof-of-concept testing with a near IR pulse laser was also performed, successfully initiating failure in pouch and cylindrical cells with a minimal energy input.					
<b>17. Key Words</b> Thermal runaway, pouch cell, lithium-ion battery, Li-ion battery			<b>18. Distribution Statement</b> This document is available to the public through the National Technical Information Service, <a href="http://www.ntis.gov">www.ntis.gov</a> .		
<b>19. Security Classif. (of this report)</b> Unclassified		<b>20. Security Classif. (of this page)</b> Unclassified		<b>21. No. of Pages</b> 29	<b>22. Price</b>

Form DOT F 1700.7 (8-72)

Reproduction of completed page authorized

# Table of Contents

Table of Figures .....	iii
Objective .....	1
Summary .....	1
High-Intensity Light Source (Quartz Lamp).....	1
Laser Battery Failure Initiation.....	5
Thermite Initiator Development.....	10
NSWC Carderock’s Commercial Thermite Testing.....	13
Test Procedure .....	14
Results.....	15
Test #1.....	15
Test #2.....	16
Test #3.....	17
Test #4.....	19
Test #5.....	20
Conclusions .....	21

## Table of Figures

Figure 1. Design and images of quartz lamp testing apparatus.....	2
Figure 2. This figure shows the measured heat flux from a cell under thermal runaway as measured through Accelerating Rate Calorimetry. This is used to develop a simulated heat flux profile with the final developed profile also shown.....	2
Figure 3. The external cell temperature (TC5) is shown along with the heat flux applied by the quartz lamp. This shows insufficient heating to initiate thermal runaway with the applied simulated profile.....	3
Figure 4. Revised profile shown alongside data from Figure 2.....	3
Figure 5. Results of testing with revised quartz lamp heating profile showing thermal runaway of target cell.....	4
Figure 6. Surface of cell after revised profile. Note extensive damage from exposed area.....	4
Figure 7. Internal damage of cell after revised profile. Note even current collectors are significantly damaged in the target area. ....	5
Figure 8. Setup of laser initiation testing on pouch cells before and after cell runaway. Initial testing was performed on unconstrained cells; however, constraint was also deemed viable.....	6
Figure 9. Thermal runaway results of initial proof-of-concept laser initiation testing with pouch cells.....	7
Figure 10. Comparison of nail penetration testing (left) to laser testing (right) .....	7
Figure 11. External images and X-Ray radiographs comparing damage from laser initiation on a discharged cell and nail penetration on a similar pouch cell. Top left shows the impact of the low-power laser on the surface of a discharged cell, repeated on the cell using the same power settings that were able to initiate thermal runaway. Bottom left shows CT imaging showing the internal damage of this result. Top right shows the puncture made with a nail penetration test typically used to initiate thermal runaway. Bottom right shows the aftermath of thermal runaway caused by a nail penetration test, showing the macro-scale damage to the cell from the nail.....	8
Figure 12. Failure initiation on a cylindrical LCO cathode cell. Full discharge was observed but no high-rate runaway. Two surface thermocouples were measured on either side of the nail target (TC1 and TC2) .....	9
Figure 13. Failure initiation on a cylindrical NCA cathode cell. A high-rate runaway of the cell was observed in this case.....	9
Figure 14. Initial test crucibles for custom thermite initiation cartridges.....	10
Figure 15. A diagram of the test setup of the custom crucible testing. ....	11
Figure 16. Heating profile results of the Al/MnO <sub>2</sub> thermite tests. ....	12
Figure 17. Heating profile results of the Ti/2B thermite tests.....	12
Figure 18. Damaged crucible shown after Ti/2B tests.....	13
Figure 19. AA Portable Power Corp Li-ion Polymer Pouch Cell .....	13
Figure 20. Cadweld Thermite Caps .....	13
Figure 21. Cadweld Plus Control Unit .....	14
Figure 22. Test setup picture for test #1: (a) top view, (b) side view. ....	15
Figure 23. Temperature graph for one of the runs of test #1. The temperature of the crucible’s bottom peaked at 210°C.....	15
Figure 24. Test setup picture for test #2.....	16

Figure 25. Temperature graph for one of the runs of test #2. The bottom of the thermite cap peaked at 1200°C..... 16

Figure 26. General test setup for tests 3 to 5. .... 17

Figure 27. Setup pictures for test #3..... 17

Figure 28. Temperature graph for one of the runs of test #3. Peak cell temperature was 220°C. .... 18

Figure 29. Temperature graph for one of the runs of test #4. Cell went into thermal runaway and temperatures peaked at 650°C..... 19

Figure 30. Setup picture for test #5. .... 20

Figure 31. Temperature graph for one of the runs of test #5. Top cell temperatures peaked at 350°C while the bottom cell only reached to 50°C. .... 20

## Objective

This project aims to advance the state of the art of lithium-ion battery thermal runaway propagation testing by exploring novel single-cell failure initiation and simulation methods. This report details testing progress to date.

## Summary

As increasingly complex lithium-ion systems are used, a specific concern has arisen surrounding thermal runaway propagation. Specifically, the concern is that a random field failure of a single cell could cause a cascading failure of other nearby, otherwise healthy, batteries that ultimately consumes a significant portion of the system. Once systems are comprised of large numbers of cells, the likelihood of a catastrophic failure can increase if this failure overcomes the entire system. Testing to date has largely focused on single-cell initiation using traditional abuse test methods. However, these methods raise concerns either with the amount of impact to the overall system, or the difficulty in performing the test in a pack outside of a research and development setting.

This project looks at novel initiation methods applied to either initiate or simulate the failure of a single-cell test. Specifically, it explores first initiation with a high-intensity, undirected light source, a high-intensity quartz lamp. This method successfully initiated thermal runaway in pouch cells. However, energy input to the cell similar to the requirement for resistive heating was needed. In addition, this method was found to only be applicable with the large face of prismatic and pouch cells, limiting the convenience of the technique.

Testing was also performed to develop a contained thermite test device. Commercial thermite materials tested at NSWC Carderock successfully initiated thermal runaway within a single cell. However, to limit impact to the surrounding system, a contained testing device is desired. For this reason, pellets were compacted inside tungsten crucibles and tested to obtain the desired containment and thermite reaction. However, to date no crucibles tested have could fully contain the thermite reaction, making this technique difficult outside of specialized testing laboratories. Ongoing work will make a final determination of the feasibility of a sealed thermite test device.

Proof of concept testing with a near IR pulse laser was also performed and was successful at initiating failure in pouch and cylindrical cells with a minimal energy input. This method currently shows most promise for further exploration. Next year's work will focus on fully exploring the feasibility of this technique.

## High-Intensity Light Source (Quartz Lamp)

Initial studies attempted to create a single-cell thermal runaway by heating a small area with a quartz lamp. Radiation was masked from a high-intensity light source with cement board to limit the flux to a controlled 2.5 cm diameter aperture area. The general setup is shown in Figure 1. The duration and intensity of the flux were controlled to attempt to match the flux coming from a single-cell failure, effectively mimicking the heat flux that would be experienced by a single cell if the nearest neighbor cell

went into thermal runaway. The values of this heating profile were determined based on values taken from accelerating rate calorimetry (ARC) shown in Figure 2 and the heat flux output calibrated with measurements from an infrared radiative flux meter, with the resulting profile also shown in Figure 2.

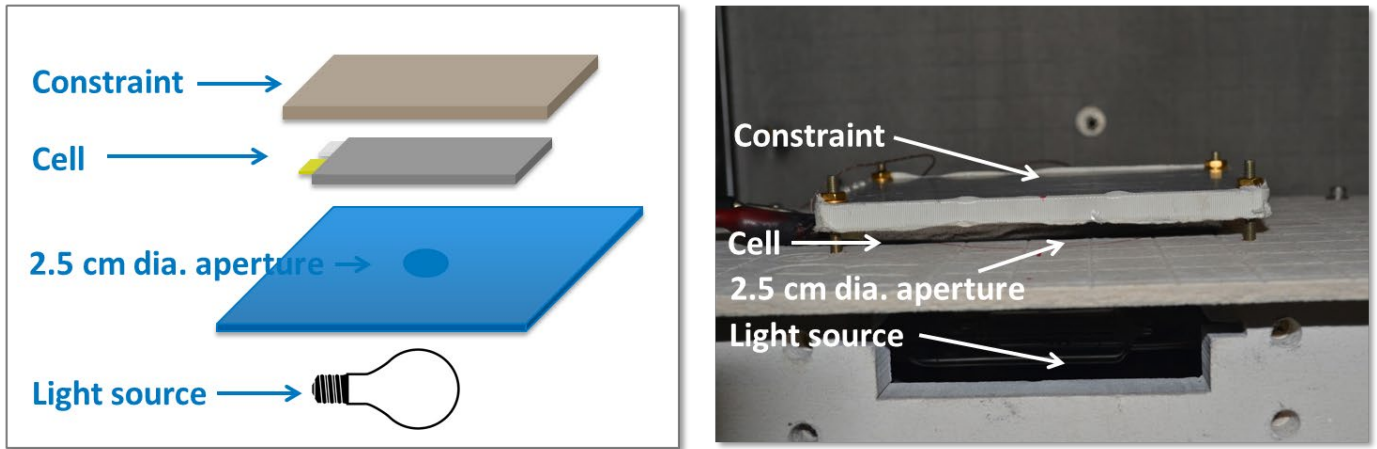


**Figure 1.** Design and images of quartz lamp testing apparatus

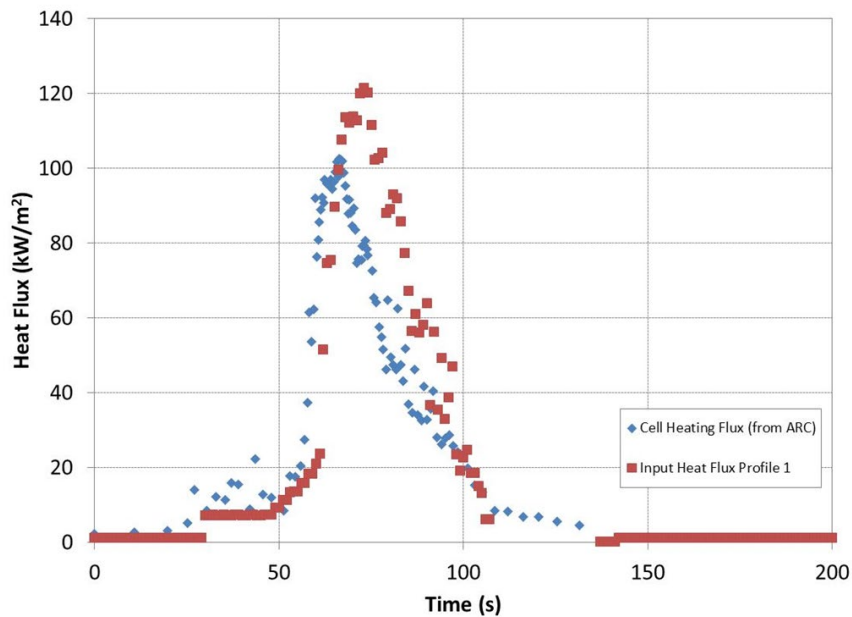


**Figure 2.** This figure shows the measured heat flux from a cell under thermal runaway as measured through Accelerating Rate Calorimetry. This is used to develop a simulated heat flux profile with the final developed profile also shown.

Initial testing with the calibrated profile is shown in Figure 3. It shows that the initial calibrated profile could not send the cell into thermal runaway, with temperatures of the cell nearest to the aperture showing a peak of just under 70 °C. Subsequently, a new profile was developed for further testing. This is shown and compared to the previous profile in Figure 4. This new profile doubled both the duration and the intensity of the heat flux.

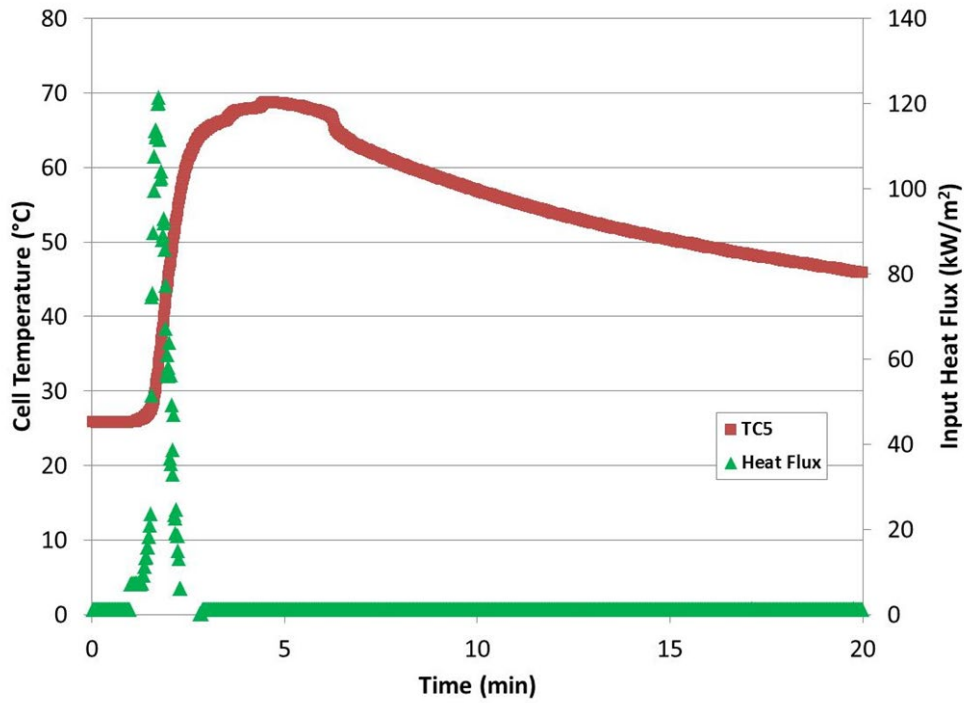


**Figure 3.** The external cell temperature (TC5) is shown along with the heat flux applied by the quartz lamp. This shows insufficient heating to initiate thermal runaway with the applied simulated profile.

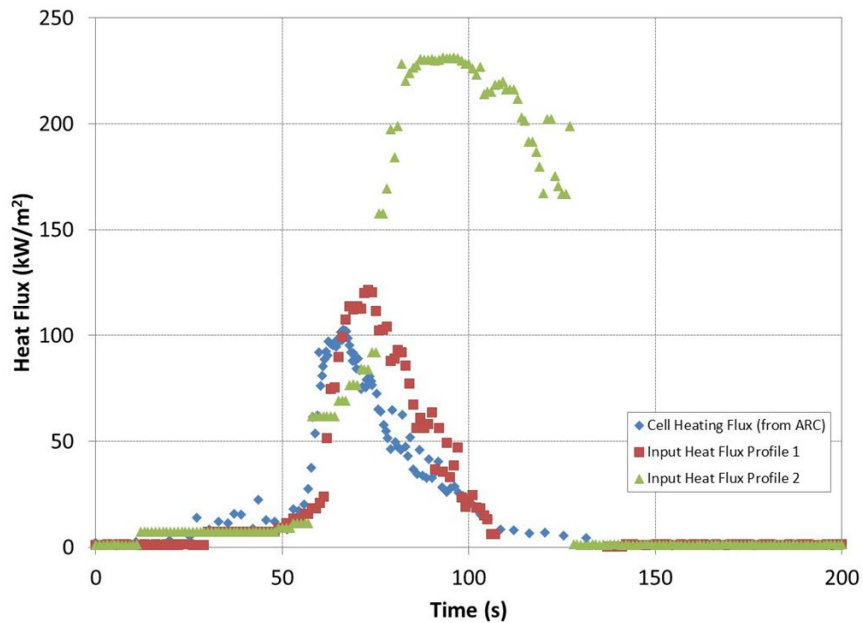


**Figure 4.** Revised profile shown alongside data from Figure 2

Results of testing with the new profile from Figure 4 are shown in Figure 5. This indicates that thermal runaway of the single cell was achieved with the new flux profile, leading to a peak temperature of ~570 °C and rapid voltage loss of the cell. Post-mortem analysis was performed on the tested cell to evaluate the extent of the damage caused to the cell (see Figures 6 and 7). Extensive damage to the target, both on the surface of the cell and extending several layers deep into the cell, was noted. Not only were the active materials damaged, but extensive damage was also done to current collectors and separators within the targeted area.

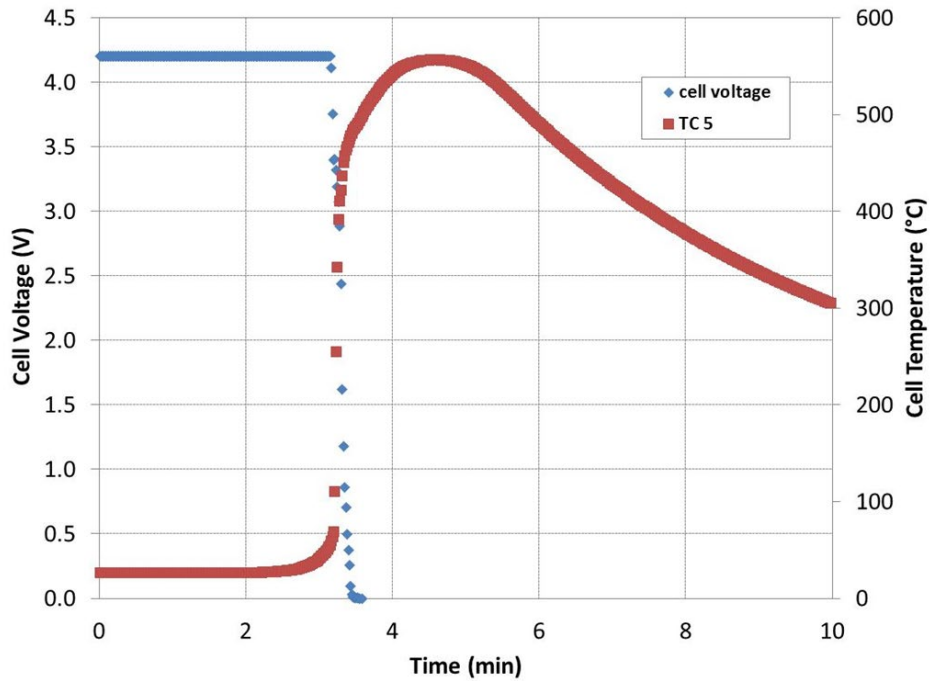


**Figure 5.** Results of testing with revised quartz lamp heating profile showing thermal runaway of target cell.

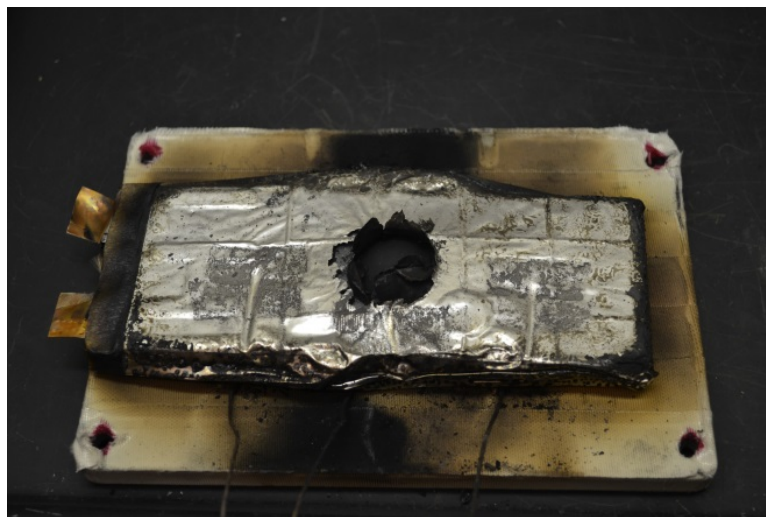


**Figure 6.** Surface of cell after revised profile. Note extensive damage from exposed area.



**Figure 7.** Internal damage of cell after revised profile. Note even current collectors are significantly damaged in the target area.

## Laser Battery Failure Initiation

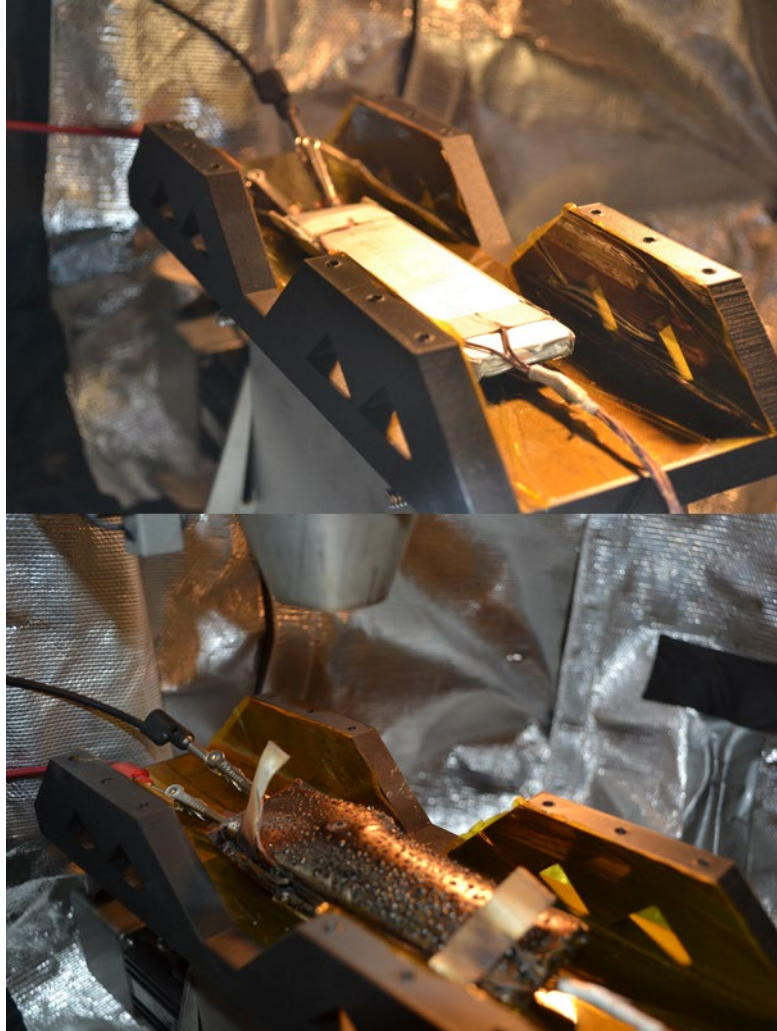
Focusing the energy from the high-intensity lamps was considered, however it seemed unfeasible to focus the undirected light. Alternatively, it was determined that a similar effect could be achieved with a commercial welding laser to create a small localized hotspot within a single cell. This work used a Rofin 40W 1000 nm (near infrared) pulse welding laser for this testing. The initial work was performed on 3 AH polymer pouch cells, 2.6 AH 18650 LCO cells and 3 AH 18650 NCA cells.

Pouch cells were placed in a cell holder set up to expose the largest face to the beam. The beam was focused to a spot size of  $\sim 1\text{mm}$  and aligned to strike in the approximate center of the target face of the cell. This setup is shown in Figure 8. This figure also shows the tested cell before and after thermal runaway from testing. Initial proof of concept work was performed on a fully unconstrained cell; however, constraint was achieved with phenolic boards with a central piece removed to allow the laser to pass through.

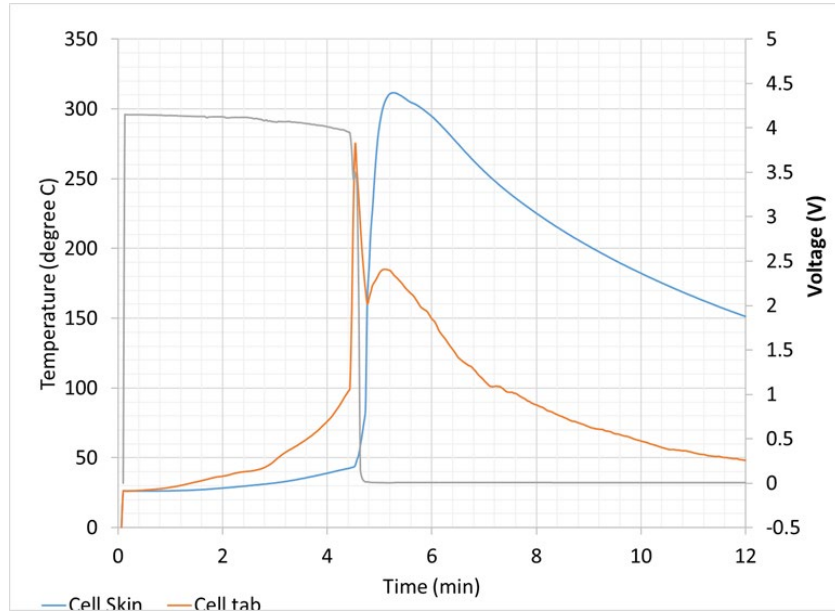
Figure 9 shows the thermal runaway created by the initial proof of concept testing on 3 AH pouch cells. It shows an initial lower rate heating process that begins shortly after the initial laser exposure. This low-rate heating continues for  $\sim 4.5$  minutes until the onset of high-rate thermal runaway occurs. This low-rate heating is accompanied by a slight voltage loss of  $\sim 200$  mV as the induced failure develops. Once high-rate thermal runaway occurs, rapid voltage loss to effectively 0V and a peak temperature of  $320^\circ\text{C}$  was observed.

Figure 10 compares the results from Figure 9 to nail penetration as the closest analog standard abuse test. The severity of the two tests in terms of peak temperature is very similar. Peak temperatures of just over  $300^\circ\text{C}$  were observed in both cases as the high-rate thermal runaway rapidly consumes the cell. This overall result is not surprising as both techniques add very little energy to the cell prior to failure and both are at roughly ambient conditions when thermal runaway occurs. The primary difference in the observed failures is in the onset and development of the failure from the initial impact

of the test. In the case of the nail penetration, thermal runaway occurs nearly simultaneously with the penetration of the nail. In addition, the thermal runaway rapidly progresses from ambient to the maximum observed temperature. The laser initiated failure, however, developed over several minutes, beginning with a low-rate self-heating event that then develops into a rapid thermal runaway.



**Figure 8.** Setup of laser initiation testing on pouch cells before and after cell runaway. Initial testing was performed on unconstrained cells; however, constraint was also deemed viable.



**Figure 9.** Thermal runaway results of initial proof-of-concept laser initiation testing with pouch cells.

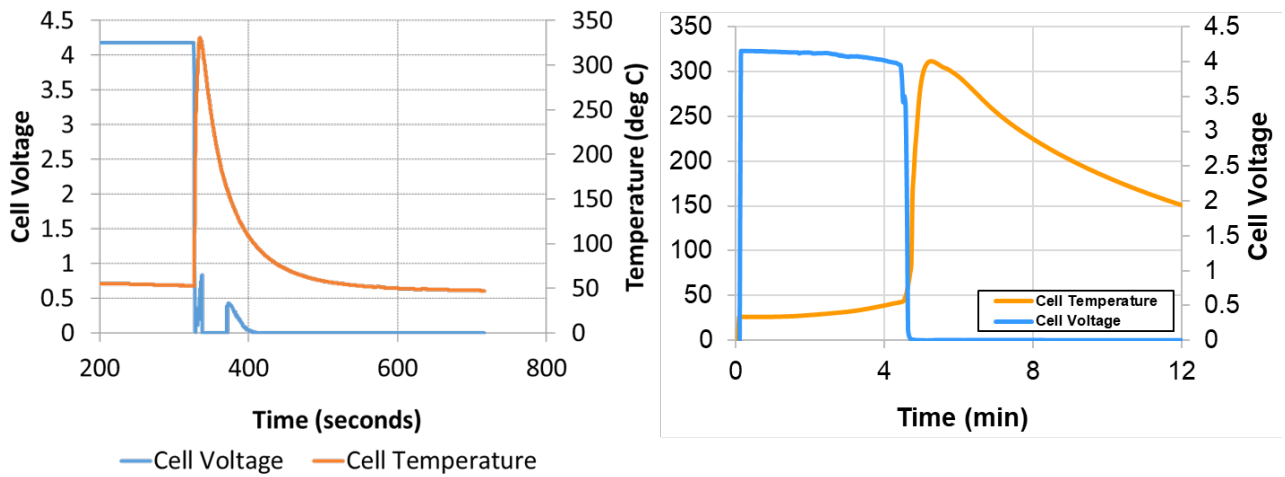


**Figure 10.** Comparison of nail penetration testing (left) to laser testing (right)

The second observed difference was in the level of physical damage to the battery. Figure 11 shows external and x-ray radiographs of the damage caused by both the laser (left) and 3mm blunt nail (right). The laser testing in this case was performed on discharged cells to provide easy identification of damage caused by the laser. This shows a significant difference in the extent of damage during nail penetration, with the nail causing a large level of deformation within the cell. This damage extends deep within the cell. Meanwhile, the laser primarily affects the surface layers of the cell. A full physical teardown was performed as well. Images provided in Appendix A. The radiographs and teardown show that the primary impacts are to the first few layers of the cell stack, with the damage only penetrating the first 3-5 layers. This limits the damage caused by the test, but also illustrates that it is primarily limited to surface damage, with impacts deep into the cell stack potentially difficult.

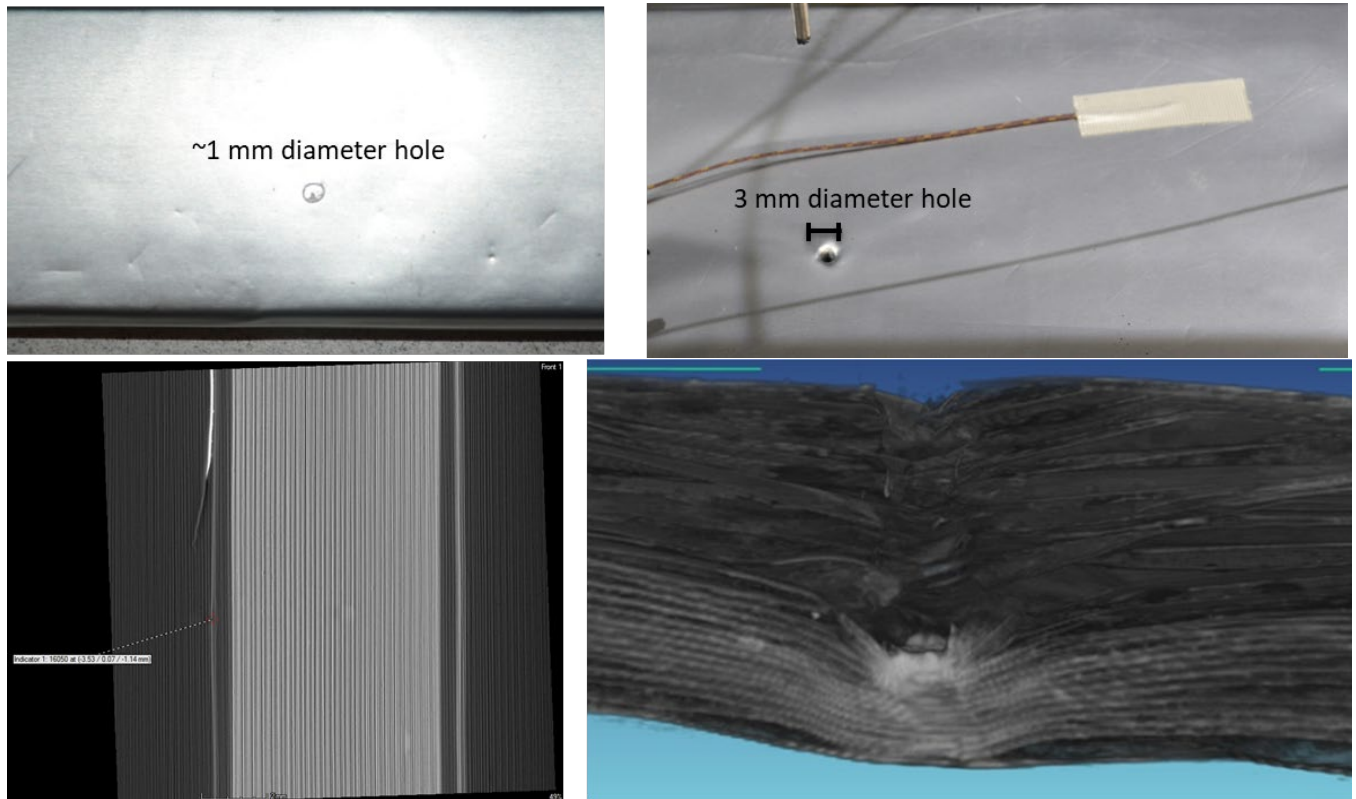


**Figure 11.** External images and X-Ray radiographs comparing damage from laser initiation on a discharged cell and nail penetration on a similar pouch cell. Top left shows the impact of the low-power laser on the surface of a discharged cell, repeated on the cell using the same power settings that were able to initiate thermal runaway. Bottom left shows CT imaging showing the internal damage of this result. Top right shows the puncture made with a nail penetration test typically used to initiate thermal runaway. Bottom right shows the aftermath of thermal runaway caused by a nail penetration test, showing the macro-scale damage to the cell from the nail.

Figures 12 and 13 show initial testing performed on LCO (Figure 12) and NCA (Figure 13) 18650 cells respectively. Cylindrical cells proved more difficult to initiate thermal runaway, requiring some preparation for testing. Care was taken during alignment to ensure a direct target for the beam. The surface was painted black to increase the absorptivity of the surface and ensure failure. The lower energy LCO cell (Figure 12) showed a significantly more limited response to the failure, with an initial temperature rise of up to 50 °C. This behavior is consistent with the development of a resistive internal short, with the voltage gradually decaying over ~10 minutes, maintaining an elevated temperature over this time but not progressing into thermal runaway. The NCA cell meanwhile, exhibited a high-energy thermal runaway with maximum temperatures approaching 700 °C. There is currently not enough information to conclusively determine the reason for the different behavior, as while NCA is known to have more energetic failures, the cell constructions may have been different as well. Current work is exploring various iterations of the laser initiation method to better understand how it may be applied as a propagation testing initiator.

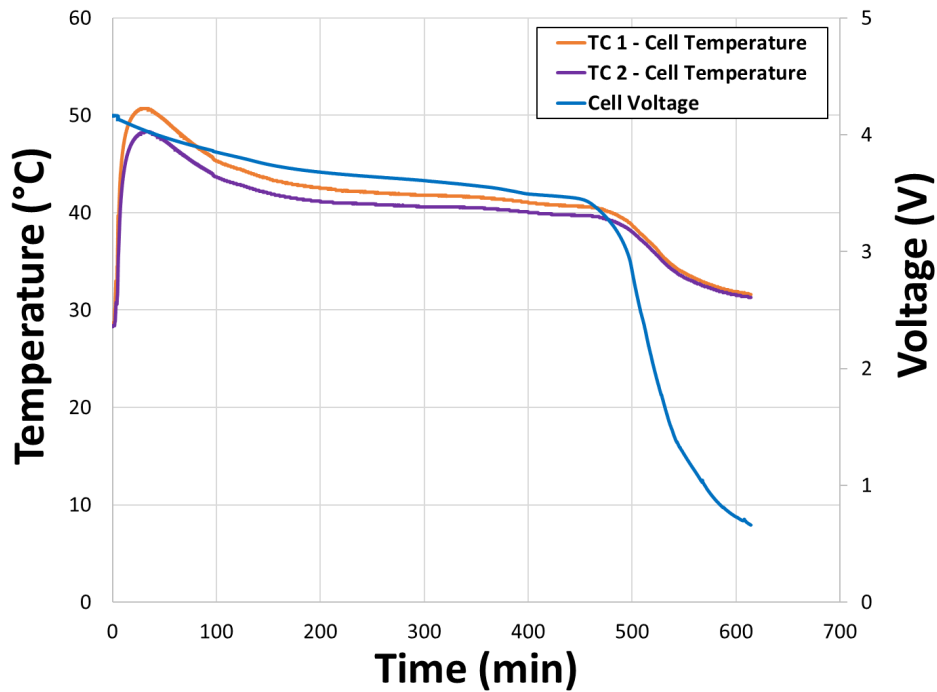


**Figure 12.** Failure initiation on a cylindrical LCO cathode cell. Full discharge was observed but no high-rate runaway. Two surface thermocouples were measured on either side of the nail target (TC1 and TC2)

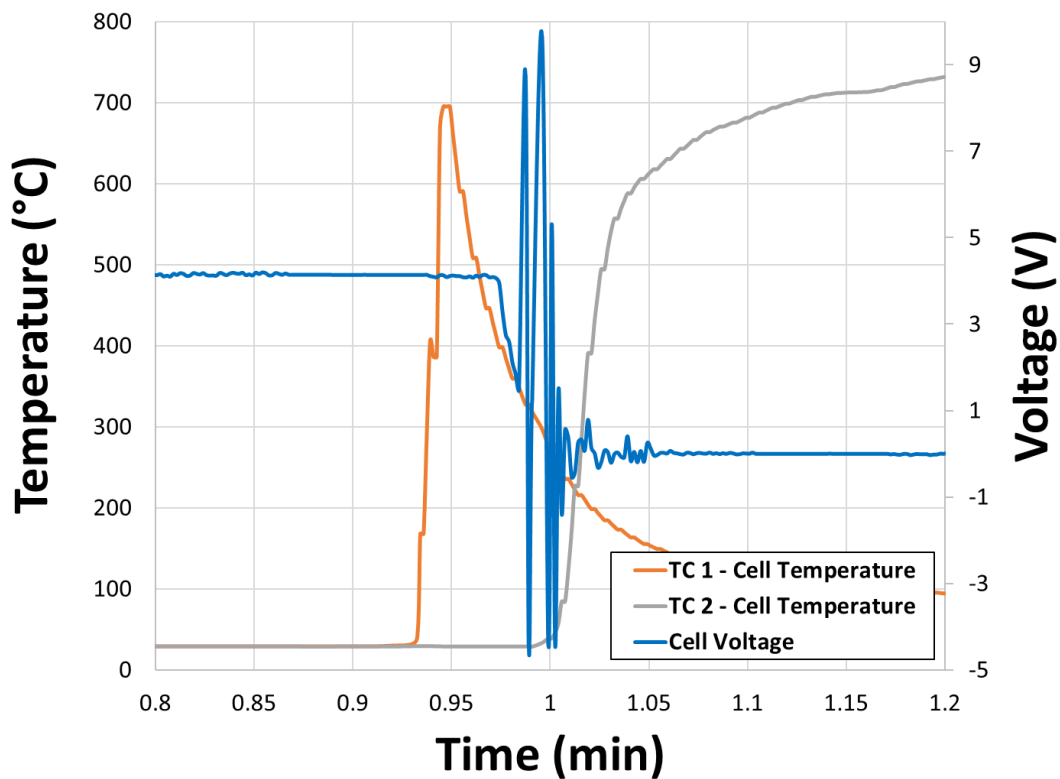


**Figure 13.** Failure initiation on a cylindrical NCA cathode cell. A high-rate runaway of the cell was observed in this case.

## Thermite Initiator Development

Work has been ongoing at Sandia to develop a thermite-based chemical initiator that would be able to simulate the thermal runaway of a single cell in a small contained device. The original design used a tungsten crucible to attempt to contain the thermite reaction. The original material chosen was the Al/MnO<sub>2</sub> thermite system as a thermite chemistry with sufficient heating rates to match those seen in single-cell thermal runaway tests (see ARC data accompanying high-intensity light testing above). Figures 14 and 15 show the general design of the crucible and the experimental setup for initial testing. Initial testing was performed within a standard test chamber to determine if the crucible would be able to adequately contain the reaction.

The Advanced Power and Energy Branch (Code 636) of the Naval Surface Warfare Center Carderock Division (NSWCCD) investigated the viability of using commercial thermite as an initiation method for thermal runaway for pouch cells. Thermite is a pyrotechnic composition that contains a metal and metal oxide powder. It is stable at room temperature and can only be ignited under extreme temperatures. When ignited, thermite undergoes an exothermic reaction where the metal reduces the metal oxide. The reaction is able to generate significant heat (over 4,000°F) in a short period of time.

Thermite is a viable material for the simulation of a single-cell thermal runaway initiative (SCTRI) since it produces high heat, and can be engineered to mimic the heat release of a cell failure by varying the formulation and quantity. The thermite reaction can be further controlled to get the desired heat release rate over time by distributing the thermite throughout a binder material in such a way as to produce a thermite chain reaction.

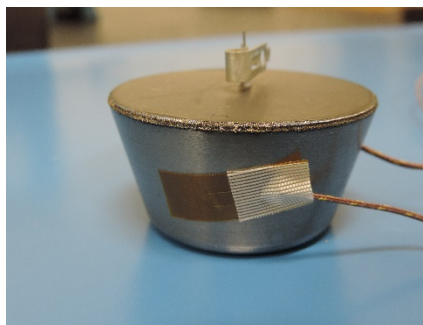


**Figure 14.** Initial test crucibles for custom thermite initiation cartridges.

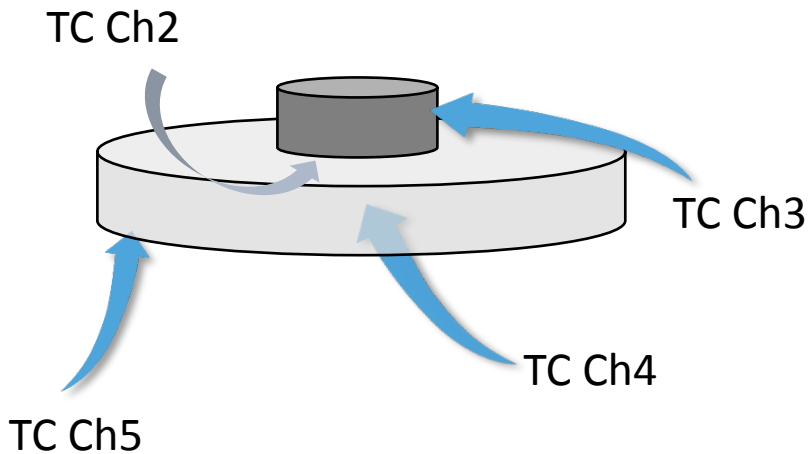


**Figure 15.** A diagram of the test setup of the custom crucible testing.

The heating profiles observed during testing of the Al/MnO<sub>2</sub> materials are shown in Figure 16. The initial heating rates were promising, although potentially insufficient to induce thermal runaway at these levels. However, further refinement of this chemistry was not performed as the gas generation was sufficient to destroy the crucible and breach containment. This material system was abandoned as being likely too severe of a gas generating chemistry to be useful. Videos of the testing showing this problem are available as supplemental material to this report.

Further materials were explored at this point and it was determined that the Ti/2B system was a promising candidate due to low theoretical gas generation. This material was pressed into the same design of crucible as seen in Figures 14 and 15 above. Figure 17 shows the resulting heating profiles. These show higher temperature heating profiles than the Al/MnO<sub>2</sub> system, with peak temperatures approaching 240 °C that would more readily induce thermal runaway within an adjoining cell to the device. However, similar issues were found with the containment within the crucible, with the lid of the crucible cracking and separating from the main body allowing thermite to erupt from the device. An image of the crucible that was taken after the test is shown in Figure 18 and video of this test is available as supplemental material to this report.

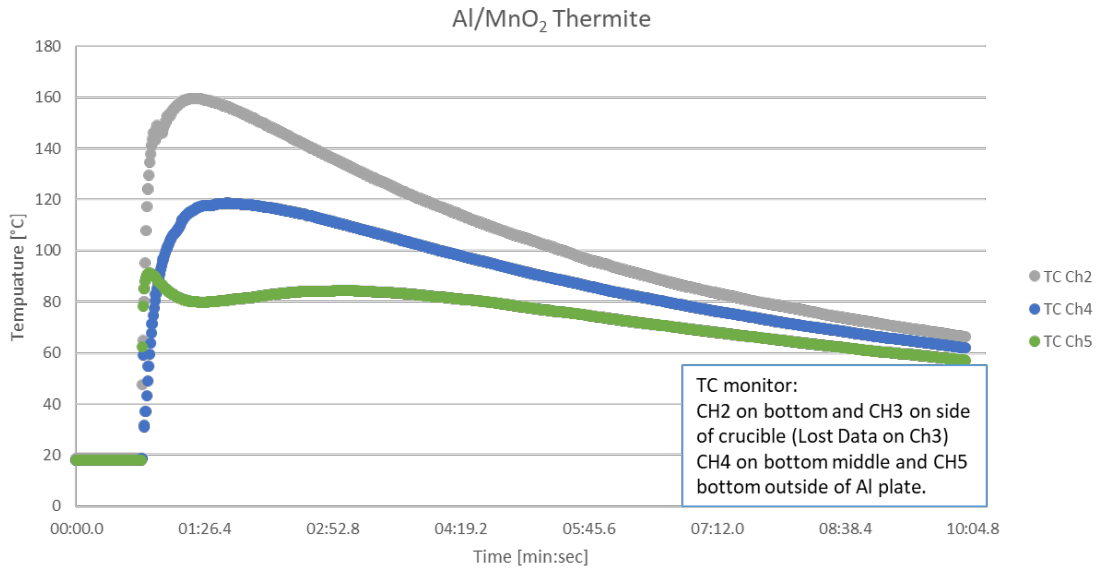


**Figure 16.** Heating profile results of the Al/MnO<sub>2</sub> thermite tests.

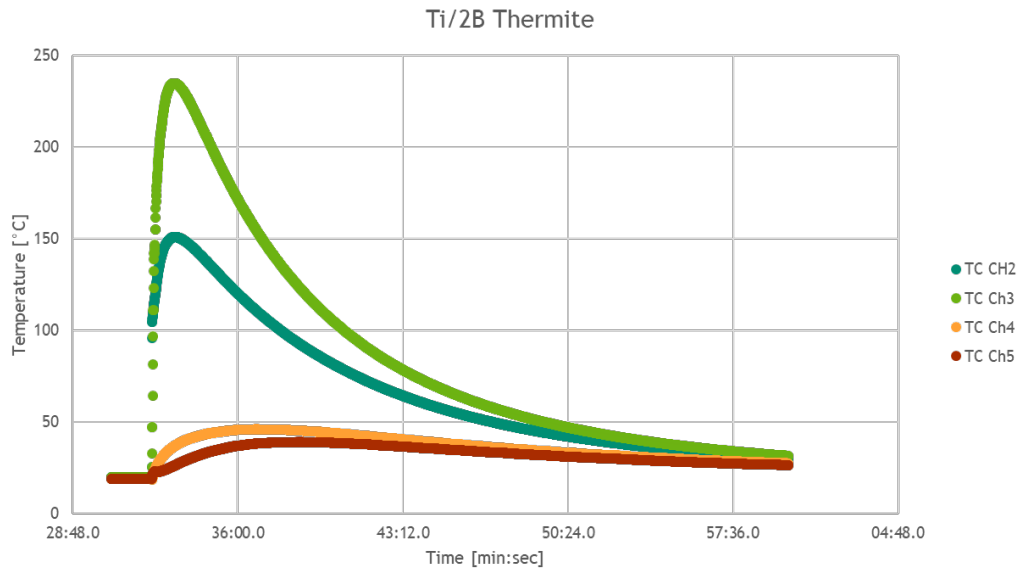


**Figure 17.** Heating profile results of the Ti/2B thermite tests.



**Figure 18.** Damaged crucible shown after Ti/2B tests.

## NSWC Carderock's Commercial Thermite Testing



**Figure 19.** AA Portable Power Corp Li-ion Polymer Pouch Cell

Testing was performed on the AA Portable Power Corp (Part Number: 8790140-2C) lithium-ion polymer pouch cell (Figure 19). It has a lithium nickel manganese cobalt oxide ( $\text{LiNiMnCoO}_2$ ) cathode with a nominal voltage of 3.7 V and 10 Ah capacity, for a total energy content of 37 Wh. The cell dimensions are 141.2mm x 91mm x 9.2mm and weighs 240 g.



**Figure 20.** Cadweld Thermite Caps

The commercial thermite product used is a Cadweld brand thermite. Cadweld thermites are premixed, portions of  $\text{Cu}_2\text{O}$ ,  $\text{CuO}$ ,  $\text{Cu}$ , and  $\text{Al}$  powder in a sealed plastic cap (Figure 20). The caps have an igniter

strip on top and can be remotely started with a Cadweld Plus Control Unit (Figure 21). The caps have an auto-ignition temperature of 1,750°F. The caps used specifically are the 15PLUSF20 that are color coded with a black ring on top. The cap weighs 49 g and contains about 15 g of thermite powder.



**Figure 21.** Cadweld Plus Control Unit

## Test Procedure

Testing was as follows:

Test #	# of Battery Cells	# of Tests	Test Name
1	-	2	Test of thermite cap on crucible
2	-	3	Test of thermite cap without crucible
3	2	2	Thermite cap on top of cell 0%SOC
4	3	3	Thermite cap on top of cell 100%SOC
5	6	3	Thermite cap on top of cell stack (0% SOC on top of 100%SOC)

Test #1 and 2 was run to gauge the heat generated from the thermite alone. Tests #3 and 4 were performed with the thermite cap on top of a cell at two different states of charge (SOC). Test #5 was performed after the results of tests #3 and 4 to determine if the molten metal generated from the thermite is penetrating through the top cell down to the bottom cell.

Thermocouples were used during each test to measure the temperature of the cell, thermite, and ambient atmosphere. Voltage sense lines were also used to measure the voltage of the cell. Thermocouple and voltage readings were recorded using an Agilent 34972A.

## Results

### Test #1

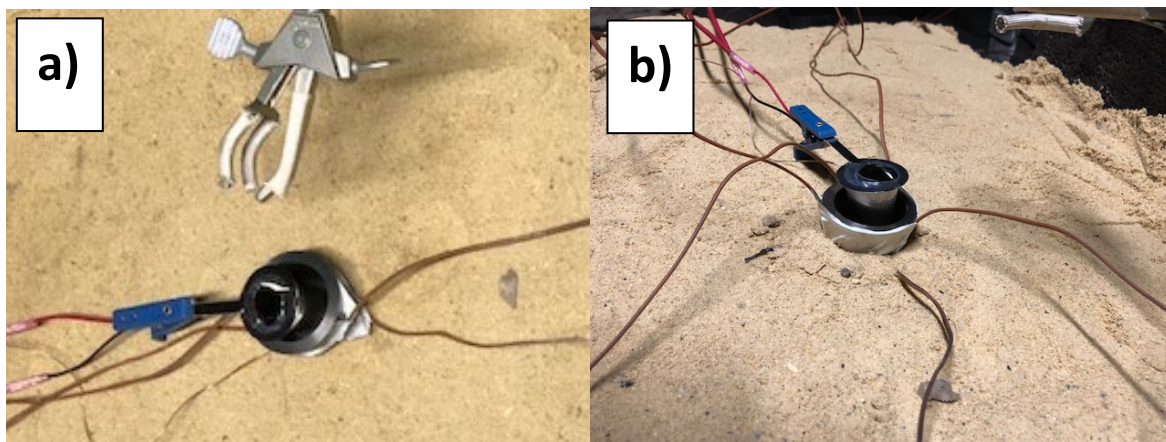


**Figure 22.** Test setup picture for test #1: (a) top view, (b) side view.

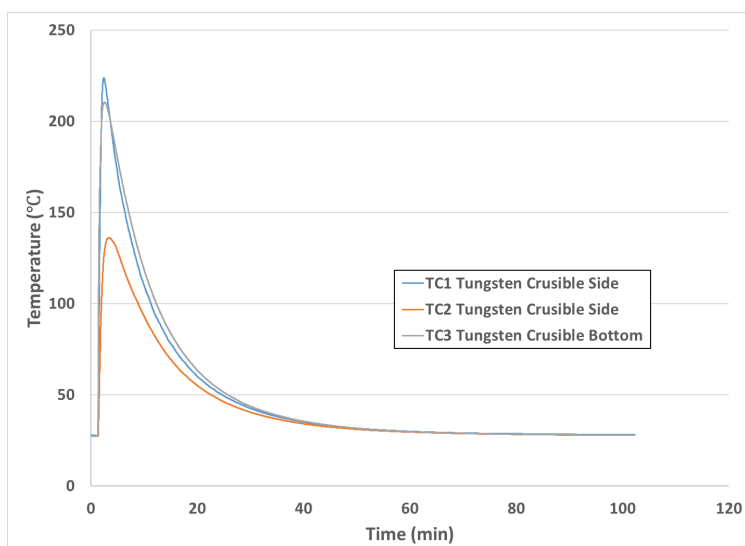


**Figure 23.** Temperature graph for one of the runs of test #1. The temperature of the crucible's bottom peaked at 210°C.

Thermocouples were placed on the side and bottom of the crucible. The crucible was placed on top of a tray of sand and held in place with a three-prong clamp (Figure 22). Results show that temperature of the crucible reached only 210°C (Figure 23). It was suspected that because of the large thermal mass the crucible had, the heat was being absorbed by the crucible itself and will not transfer over to the cell. In addition, the molten metal that is formed due to the thermite reaction adhered to the crucible and was difficult to remove. Thus, the crucible was removed and only the thermite cap was used for subsequent tests.

## Test #2

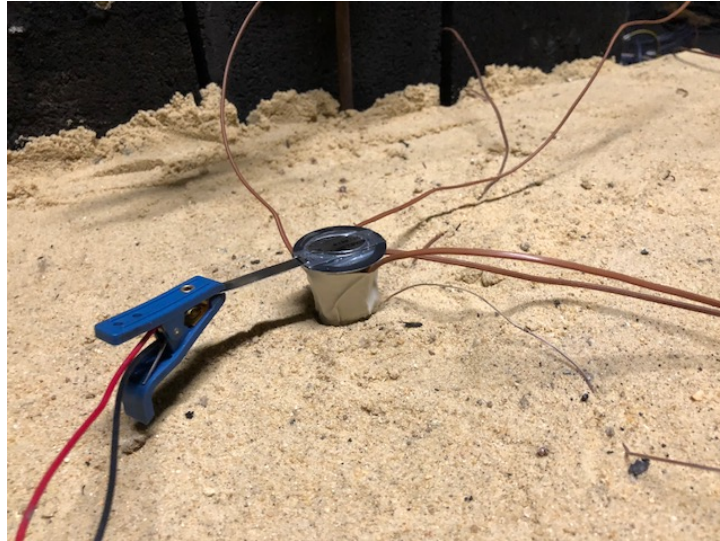


**Figure 24.** Test setup picture for test #2.

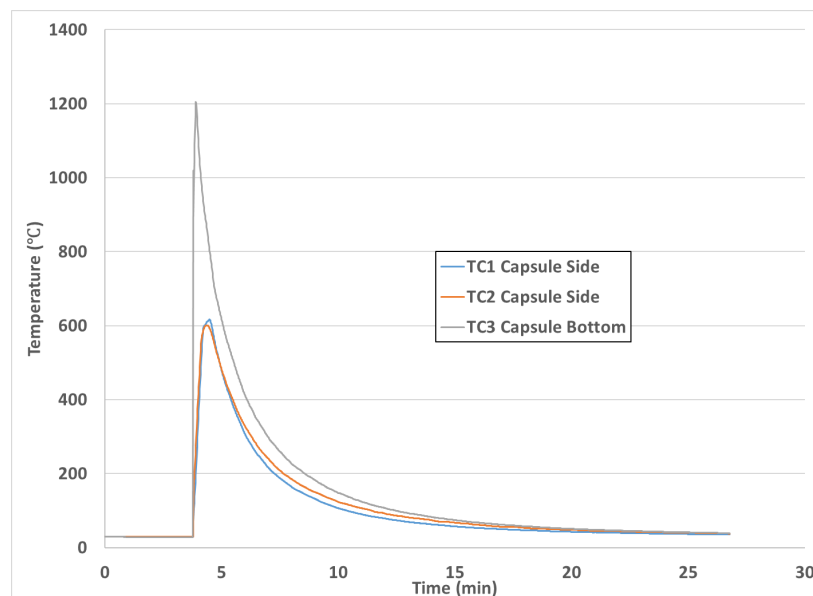


**Figure 25.** Temperature graph for one of the runs of test #2. The bottom of the thermite cap peaked at 1200°C.

Test #2 was setup in the same way as test #1 (Figure 24) with the crucible removed. Figure 25 shows example results from test 2, where the thermite cap (top of cap) was able to reach 600 °C while the bottom reached upwards of 1200 °C.

Test #3

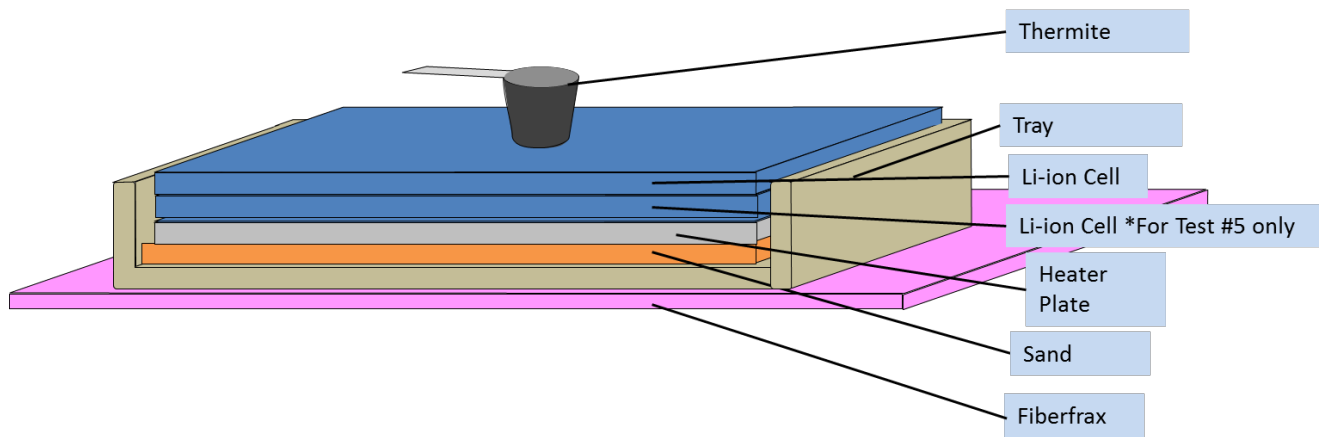


Figure 26. General test setup for tests 3 to 5.

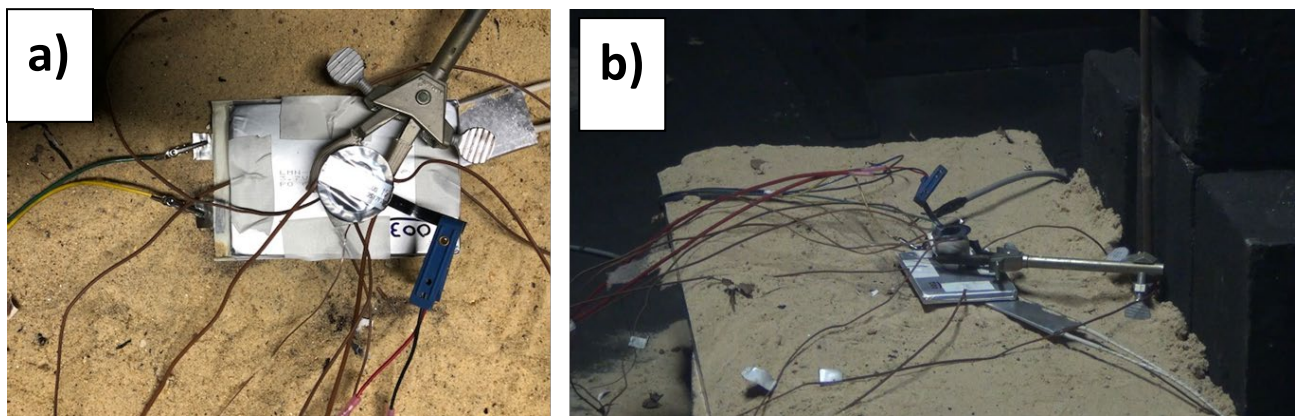
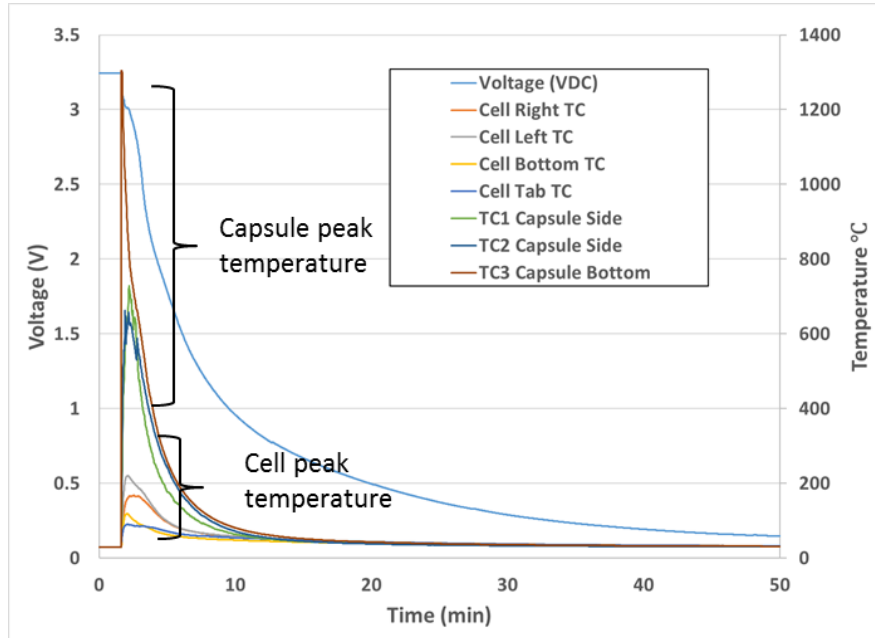


Figure 27. Setup pictures for test #3.



**Figure 28.** Temperature graph for one of the runs of test #3. Peak cell temperature was 220°C.

Test #3 setup was the same as the previous setup with the addition of a Li-ion and a heater plate underneath the thermite cap as shown in Figure 26 and Figure 27. The cell was cycled three times and then left at 0% SOC. Four additional thermocouples were placed on the edges of the cell. The heater plate underneath the cell is a render safe and is not used for the test. After the thermite was ignited, the molten metal penetrated the cell but the cell did not go into thermal runaway. Results were the same for the repeated test. From Fig 28, the peak temperature of the cap exceeded 1,200°C but the cell temperature reached only 220°C. Post analysis shows that the molten metal appears to penetrate through 5 to 7 layers of electrode material.

## Test #4

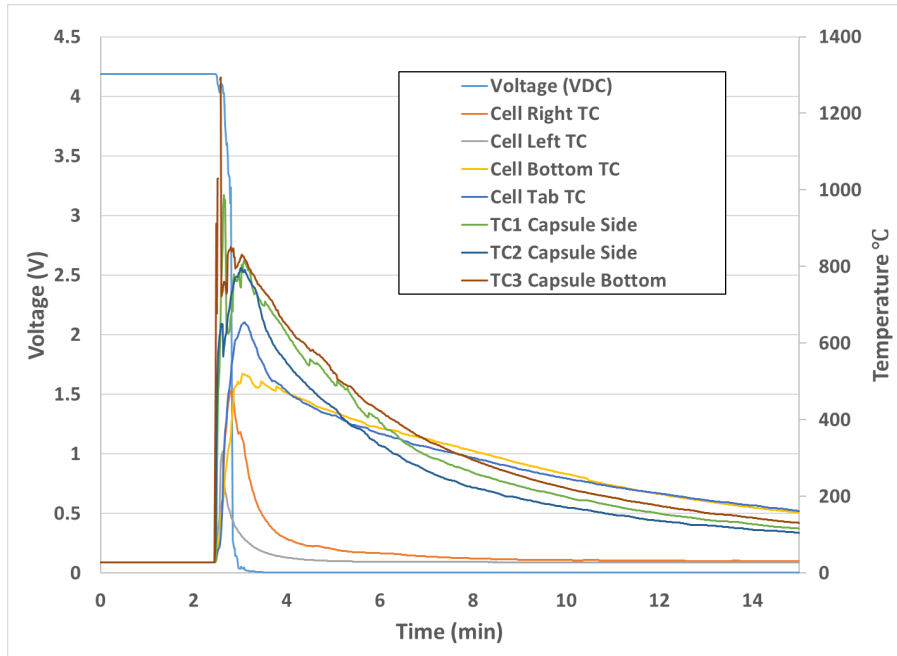


**Figure 29.** Temperature graph for one of the runs of test #4. Cell went into thermal runaway and temperatures peaked at 650°C.

Test #4 repeated test #3 with cells at 100% SOC instead of 0% SOC. A few seconds after triggering the thermite cap, the cell began to quickly expand and then burst from several sides of the cell. Because the cell is a pouch cell instead of a cylindrical cell, the cell was not able to build up enough pressure to cause the cell to eject and fly across the room (this is primarily due to the less robust pressure sealing of pouch cells). Unlike results from test #3, cell temperatures reached up to 650°C (Figure 29). Repeated testing yielded similar results.

Test #5

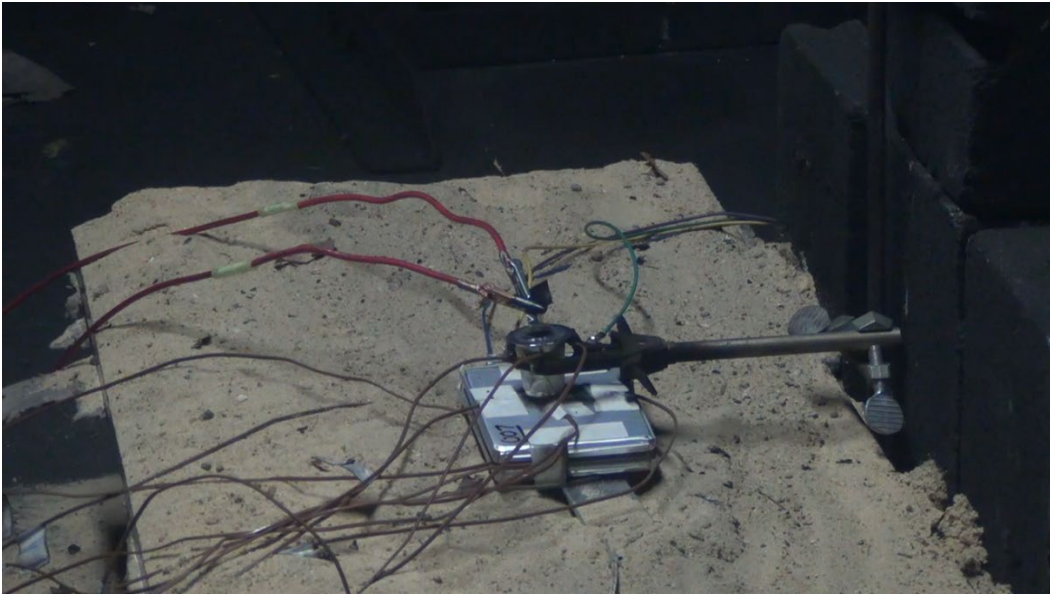


**Figure 30.** Setup picture for test #5.

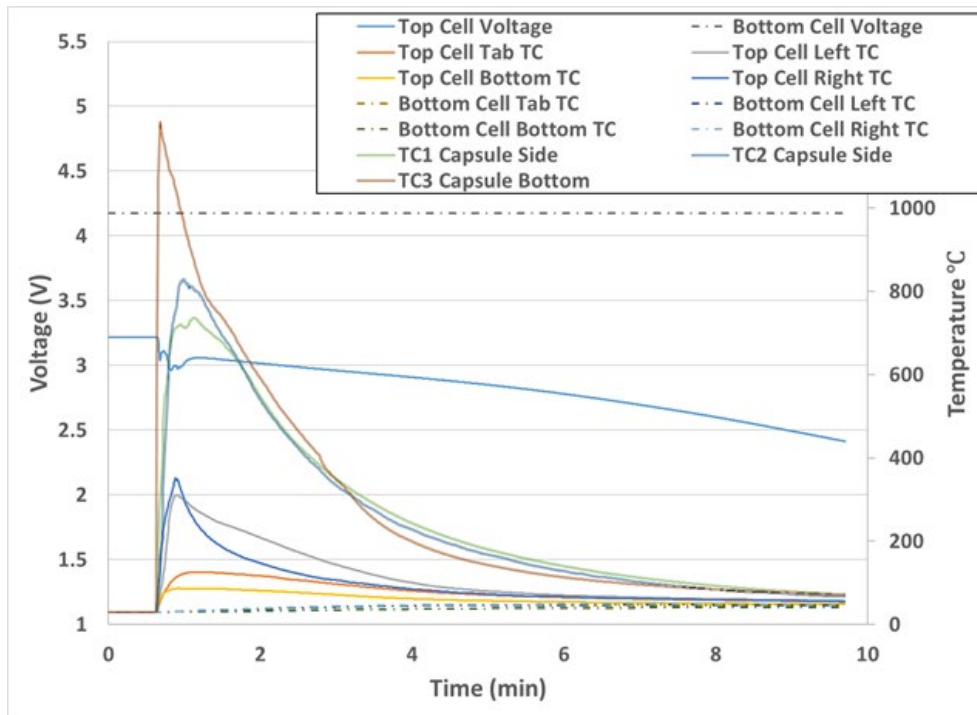


**Figure 31.** Temperature graph for one of the runs of test #5. Top cell temperatures peaked at 350°C while the bottom cell only reached to 50°C.

Test #5 was conducted to determine if the heat generated by the thermite was causing non-neighboring cells to go into thermal runaway. For this setup (Figure 26, Figure 30), a thermite cap was placed on top of two cells. The cell closest to the thermite cap was at 0% SOC while the cell further away was at 100%SOC. After the thermite was triggered, the top cell burned from the molten metal similar to the case in test #3. However, the bottom cell did not go into thermal runaway. Figure 31 shows that the top cell reached 350°C while the bottom cell reached 50°C. The test was repeated two more times with similar results.

## Conclusions

The work presented here describes testing carried out at Sandia National Laboratories and NSWC Carderock on alternative methods for single-cell thermal runaway initiators. The ultimate goal of this work is to determine alternate methods that provide an opportunity to initiate or simulate runaway of a single cell as part of a propagation test that minimizes impact to the broader pack beyond the effects of a single-cell thermal runaway event. The primary goals are to minimize physical intrusion and to either minimize energy added to the cell/pack or to create a thermal event that adequately mimics the thermal impacts of a single-cell runaway. The work presented here looks at studies in undirected light sources, thermite chemical initiators (both custom crucibles and commercial thermite sources) and proof of concept testing using an IR-fiber-coupled welding laser.

The undirected light initiation could initiate thermal runaway within a single cell during undirected light testing. However, the initial profiles intended to mimic the energy from a thermal runaway event were unable to initiate further cell failure. The overall energy input had to be roughly doubled to drive the cell into thermal runaway, significantly increasing the total energy input into the system to begin a propagating failure. In addition, the initiation was only successful when applied to the largest face of the cell due to the large area of flux required. Ultimately, the behavior of the failure observed with this initiation method was similar to heating performed with IR heaters as well, and as such would only be recommended as a potential replacement for electrical heaters.

The early proof of concept testing with the laser initiator was successful in initiating single-cell failure in both pouch and cylindrical cells. This was compared to nail penetration both in terms the physical damage to the cell and the total energy input into the cell. Table 1 shows a comparison of the laser and undirected light methods along with estimated energy inputs for more traditional initiation methods. The lowest energy impact is nail penetration; however, the laser initiation method is similarly low. Post-mortem analysis showed that the laser initiation method impacted a smaller volume of the cell, however its effects are primarily limited to the first few layers of the surface. Current work is now exploring ways to use this method more functionally as an initiation method.

Test	Energy Source	Conditions	Estimated Energy
20 Pulse laser	IR Laser	20 1.9 J pulses	38 J
Nail Penetration	Mechanical	20 mm penetration ~200 lb peak load	1.8 J
Undirected light	Quartz lamp	Exposure to light source through aperture	6000 J <sup>1</sup>
Thermal Ramp	Thermal	Heat to 200 °C	6300 J <sup>2</sup>
Overcharge	Electrical	1C to 200% SOC	43200 J <sup>3</sup>

Thermite work with commercially available thermite chemistries in standard packets were able to initiate single cells, and testing performed shows that the heat primarily is only affecting the cell directly in contact with the thermite. However, to date we have been unable to successfully create a custom crucible that would allow for a contained failure initiation cartridge within a pack. This limits the accessibility of this initiation method as testing would need to be done in laboratories that can perform testing with flammable solids. Current work is looking at a final, more robust crucible design to attempt to contain the thermite reaction and direct the heat to the target area.

---

<sup>1</sup> Value based on measured heat flux from a quartz lamp required to initiate thermal runaway on the 3 AH cells studied here.

<sup>2</sup> Estimated energy to reach 200 °C through forced heating of the 3AH cells studied here.

<sup>3</sup> Energy to reach 200% SOC in a 3 AH, 4V cell.

DOT HS 812 786  
February 2020



U.S. Department  
of Transportation  
**National Highway  
Traffic Safety  
Administration**

